Noise performance of PbS colloidal quantum dot photodetectors

A. De Iacovo[1], C. Venettacci[1], L. Colace[1], L. Scopa[2] and S. Foglia[2]
[1]*NooEl Nonlinear optics and optoelectronics Laboratory – Department of Engineering, University Roma Tre, Via Vito Volterra, 64, 00146 Rome, Italy*
[2]*CNR, Istituto dei Materiali per l'Elettronica ed il Magnetismo, Via della Vasca Navale, 79, 00146 Rome, Italy*

We report on the noise characterization of photoconductors based on PbS colloidal quantum dots. The devices operate in the near infrared with peak responsivity exceeding 70A/W at 1.3μm at low optical intensity and low voltage bias. The large responsivity, combined with the low dark current of high resistance devices provides a specific detectivity D^* as large as 10^{11} cmHz$^{1/2}$W^{-1}. The noise characteristics are investigated by noise current spectra measured at different bias in both dark and under optical excitation. The analysis revealed the noise is clearly dominated by the flicker component above 100kHz. The noise performance is investigated at different optical intensity and for different device dimensions and voltage bias.

Efficient and sensitive photodetectors are important devices for a wide variety of applications, including optical communications, imaging, spectroscopy, security, remote sensing and metrology in several fields such as food inspection, agriculture, pharmaceutical and biology. Besides the traditional semiconductor devices, in the past ten years colloidal quantum dots (CQD) were proposed as a viable and promising approach to the fabrication of optoelectronic devices, including photodetectors[1], light emitting devices[2] and solar cells[3]. CQD are solution processed semiconductor nanoparticles that can be easily deposited by simple and low cost techniques. They exhibit unique optical properties such as very large optical absorption and size tunability that have been effectively employed for the fabrication of photodetectors operating in the UV-VIS[4], near-infrared (NIR)[5] and mid-infrared (MIR)[6] spectral ranges. In addition, colloidal quantum dots, thanks to their solution processability, allow low cost, low temperature and large area fabrication and are suitable for a wide variety of substrates, including silicon, enabling their integration with electronics[7,8].

In this work we focus on PbS colloidal quantum dot photoconductors. Photoconductive detectors attracted lot of interest for their simple geometry (resulting in easy fabrication) and their inherent gain (that increases the device sensitivity). In CQD the presence of deep traps typically produces a much longer recombination lifetime for one type of carrier (electron in PbS) thus large photoconductive gain is obtained as determined by the ratio of the carrier lifetime and the transit time[9].

After the pioneering work of Konstantatos et al.[10], where impressive results have been reported (responsivity of 2700A/W and detectivity exceeding 10^{13} cmHz$^{1/2}$W^{-1}), several photoconductive detectors have been proposed looking for a suitable tradeoff between sensitivity and speed, resorting to different ligands and engineering oxidation processes of the QDs[11-14]. In addition, efforts have been devoted to the reduction of the bias voltage[14-16], since most high performance devices were operated at voltage in the 10-100V[10,11] range. Due to their large optical response, PbS photoconductors were also exploited for practical applications[17,18].

From the application point of view, one of the most important figure of merit is the specific detectivity D^*, defined by the following equation:

$$D^* = \frac{\sqrt{AB}}{NEP} \quad NEP = \frac{i_n}{R} \qquad (1)$$

where A is the device area, B is the electrical bandwidth and NEP is the noise equivalent power given by the ratio between the total noise current i_n and the responsivity R. Detectivities in the 10^8 to 10^{13} cmHz$^{1/2}$W^{-1} were reported. D^* was commonly obtained by the measurement of the responsivity and the rms noise current at a fixed bandwidth (according to eq.1)[10,11] and sometimes evaluated assuming the noise is dominated by the shot contribution and obtaining i_n by the simple relation $i_n=(2qIB)^{1/2}$, where I is the total measured DC current[18,19]. Reported detectivity in the 10^{12}-10^{13} cmHz$^{1/2}$W^{-1} is an impressive result, being comparable with the traditional semiconductor counterpart. However, with very few exceptions, the noise performance was never investigated in detail and the dominant noise source was rarely identified. While a rich literature on noise analysis in traditional semiconductor quantum dot can be found, there is almost nothing about CQD, except for very few papers[21,22]. Liu et al. investigated noise in several different nanocrystal systems, including CdS, CdSe, ZnO and HgTe, suggested the noise primarily originates from mobility fluctuations and observed the noise is mostly associated to the to the granular nature of the nanocrystal and not to the particular material composition[21]. At the time of the present study, no paper focused on noise in PbS colloidal quantum dots can be found.

In this work we investigate the noise characteristics of PbS CQD photoconductors resorting to noise current spectra measured at different bias in both dark and under optical excitation. Detectivity is measured at different optical intensity and for different device dimensions and voltage bias.

Devices were fabricated using a commercially available PbS CQD capped with oleic acid and dispersed in toluene (Sigma-Aldrich 747076, 10mg/mL, first excitonic absorption peak at 1320 nm). Nanoparticles were precipitated by centrifugation in excess methanol, then dried in vacuum and redispersed in octane with a concentration of 0.8mg/mL. The solution was drop-casted onto 1mm^2 pre-patterned interdigitated Ti-Au contacts deposited onto SiO_2 on silicon chips with finger spacing L ranging between 1 and 20μm. Devices were dried in vacuum until full solvent evaporation;

subsequently, butylamine was deposited onto the device and let react with the PbS until full evaporation. This step was repeated several times in order to obtain a film thickness of about 150nm. Devices were finally washed in methanol. A more detailed description of the fabrication process can be found in[16].

Devices were characterized in terms of DC current-voltage characteristics in dark and under illumination at 1.3μm using a KEITHLEY 2636B source measure unit. The responsivity R was measured at 1.3μm as a function of both voltage and incident optical power. The noise characterization was performed using a FEMTO DLPCA-200 ultra-low noise current amplifier followed by a HP3588A spectrum analyzer.

DC current-voltage characteristics between -5 and +5V were measured in order to check the linear behavior in both dark and under illumination, as expected from a photoconductor and typically observed in PbS CQD on high work function metals such as Au[16,23].

The device responsivity was measured from the photocurrent I_{ph} according to:

$$R = \frac{I - I_d}{P_{in}} = \frac{I_{ph}}{P_{in}} \qquad (2)$$

where I is the total current, I_d is the dark current and P_{in} is the incident optical power. Typical plots of the dark and light current and responsivity versus bias are reported in Figure 1.

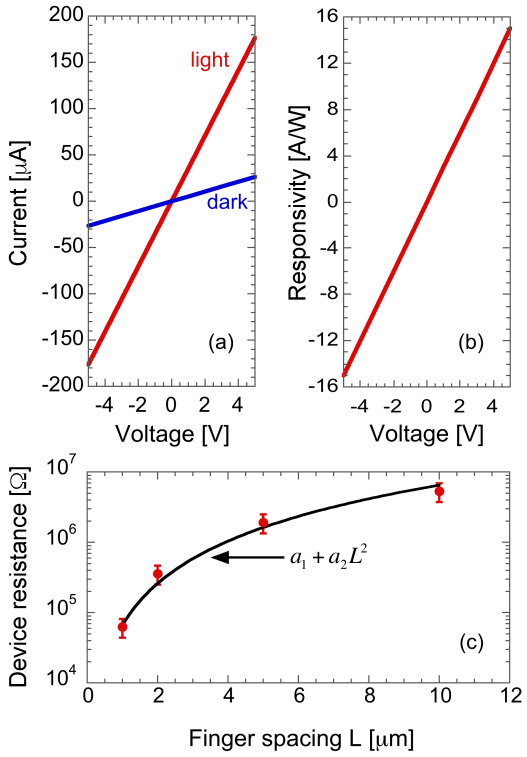

FIG. 1. Current-voltage (a) and responsivity voltage characteristics (b) with finger spacing L=1μm and Pin=50μW. Device resistance versus finger spacing (c).

Linear and symmetrical characteristics are observed. Figure 1c shows the measured device resistance R_s versus the finger spacing L. The change of the resistance is in agreement with the predicted quadratic law (as demonstrated by the fit). The L^2 scaling comes from a simple calculation of the resistance of a pair of symmetrical interdigitated contacts with variable spacing L and constant device area. The responsivity was also measured for different finger spacing of the interdigited metal contact and versus the incident optical power. Figure 2(a) shows the responsivity measured at 10nW optical power and 1V bias. The change with the finger spacing L follows the inverse squared law as expected in photoconductors[24], where the gain is proportional to the ratio between the carrier lifetime and the transit time τ_{tr} expressed as:

$$\tau_{tr} = \frac{L^2}{\mu V} \qquad (3)$$

that produces a linear dependence of the responsivity on the applied voltage (fig.1a) and the dependence on L^{-2} on the spacing L (fig.2a). Figure 2b plots the responsivity versus optical power for a 1μm spacing device biased at 1V. It exceeds 10A/W below 500nW with peak values of 70A/W in the nW range. Such behavior has been observed by other authors in similar PbS CQD devices and was associated with the dependence of the occupancy of the mid-gap states on light intensity[9,10]. The gain is promoted at low intensity when the photogenerated carrier density is lower than the trap density and electrons can be effectively trapped producing longer electron lifetime. The increase of the light intensity results in trap state filling that reduces the capture rate and consequently decreases the gain. The reported results are typical in our PbS CQD photodetectors and are useful for the following investigation on the noise performance.

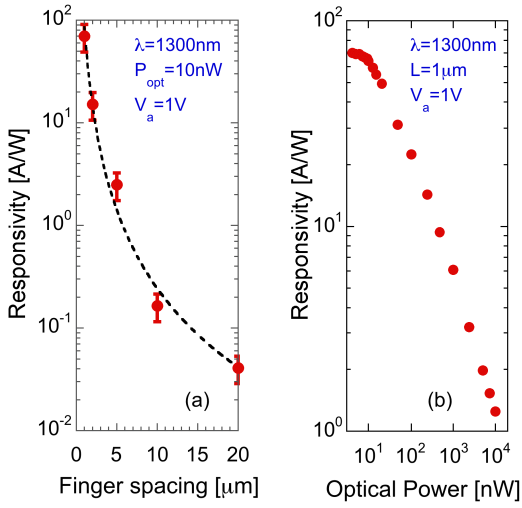

FIG. 2. Responsivity vs finger spacing (a) and versus optical power (b).

Figure 3 shows the typical noise spectra measured at 0V and at 1V bias in the 10-10^5 Hz range. The dashed lines represent the calculated shot and thermal (Johnson) noise spectral densities according to:

$$S_n^{shot} = 2qI \quad S_n^{th} = 4kT / R_s \qquad (4)$$

where q is the electron charge, I is the device current, k is the Boltzmann constant, T is the temperature in K and R_s is the device DC resistance.

With no bias the device current is zero and the spectrum closely matches the thermal noise spectral density.

When a small bias of 1V is applied, device exhibits a strong *1/f* (flicker) noise and, by extrapolation, such contribution dominates the device performance up to about 1-2MHz, where it becomes comparable with the calculated shot noise (1.7×10^{24} A^2/Hz).

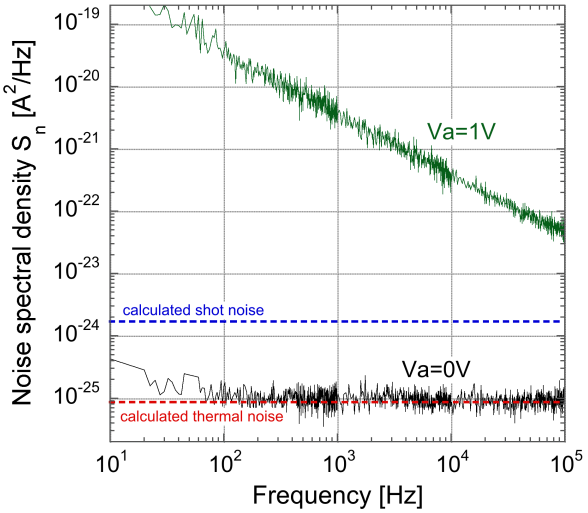

FIG. 3. Noise spectral density measured at V_a=0V (black) and V_a=1V (green). Calculated Johnson and shot noise are shown in dashed lines.

Typical noise spectra under bias are pure *1/f*, since the experimental data can be always fit by:

$$S_n^{1/f} = C\frac{I^\alpha}{f^\beta} \qquad (5)$$

with β=1±0.05.

1/f noise is always present in semiconductor devices and it is generally attributed to several independent fluctuations with an exponential distribution of characteristic times[25,26]. However, while in single crystal devices *1/f* noise is often lower than other noise sources except for very low frequency (100-1kHz), in devices based on nanocrystals it is commonly the dominant contribution over a very wide range of frequencies[27,28]. This can be associated with the granular nature of such materials, traps and defects. The large photoconductive gain and its dependence on the optical power in PbS CQD photodetectors have been attributed to the effect of traps and we believe that traps can also play an important role in noise generation; thus, we investigated the noise spectra at different bias in dark condition and under illumination.

A small portion of the noise spectra between 0.5 and 5kHz is plotted for different bias voltage in the 2-6V range, in dark and under illumination in figure 4a and 4b, respectively. In figure 4c the noise spectral density measured at 1kHz is plotted versus the corresponding current. In this way the parameter α, defined in eq.5, can be obtained by fitting the experimental data. The values for the current exponent α in dark and light conditions were 2.8±0.04 and 3.0±0.04, respectively. While α=2 is typically observed for good homogeneous resistors, we measured relatively larger values, even in devices with perfectly linear current-voltage characteristics. Such behavior has been previously observed in nanocrystals, although with different values of α (generally <2)[21,29].

It can be concluded that CQD PbS photoconductors, despite their linear I-V characteristics behave more like disordered system than homogeneous resistors.

In addition, if we compare the change of the noise spectral density versus current measured in dark and light conditions, as shown in figure 4c, we observe not only a different power law but also quite different values.

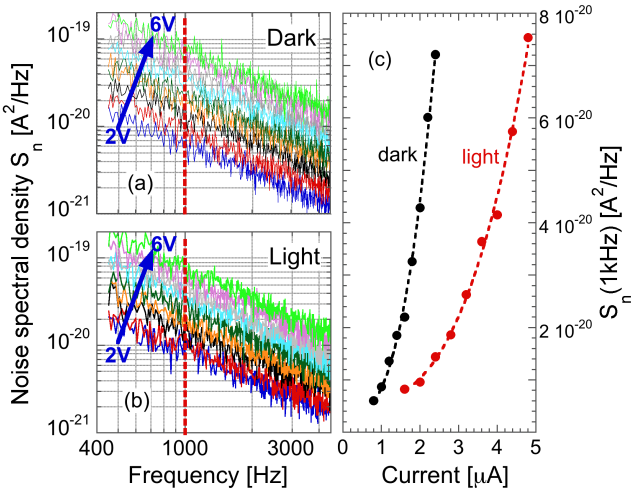

FIG. 4. Noise spectra plotted for different bias voltage in the 2-6V range, in dark (a) and under illumination (b). Noise spectral density measured at 1kHz plotted versus the corresponding current (c).

For example, the noise produced by a dark current of 2μA is five times larger than the noise produced by a photocurrent of the same value. Due to the different exponent, such difference increases at larger currents. This can be associated to the same mechanism underlying the photoconductive gain. Assuming the *1/f* noise is due to the fluctuation of the trapping-detrapping of charge carriers, it can be affected by the light intensity that changes the occupancy of the trap states.

This suggests the trap engineering can be used not only to manage the gain and the time response but also the noise and, consequently, the device sensitivity.

The device detectivity was measured according to eq.1, where the total noise current was obtained by integration of the measured noise spectral density $S_n(f)$, according to:

$$i_n = \sqrt{\int_{BW} S_n(f)\,df} \qquad (6)$$

where *BW* is the device bandwidth. *D** versus the incident optical power of devices with different finger spacing are reported in figure 5. A maximum detectivity of 10^{11} cmHz$^{1/2}$W^{-1} was obtained at 1.3μm and 1V bias in devices with 5μm spacing and using *BW*=16Hz as evaluated by $BW=(2\pi\tau)^{-1}$ with the trapping time τ obtained from a previous work[16].

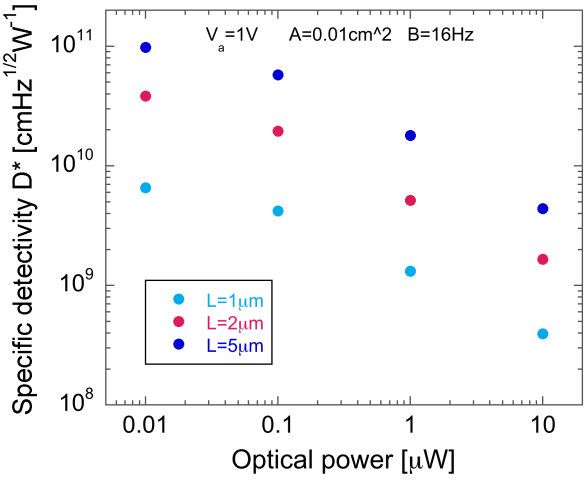

FIG. 5. Specific detectivity vs optical power for device of different finger spacing *L*.

As expected, the detectivity follows a dependence on the optical power similar to the responsivity, exhibiting maximum values at lower light intensity. In addition, devices with larger contact finger spacing exhibit larger detectivity. This is determined by the larger change of the noise current i_n with respect to the responsivity R, as shown in figure 6, where both the responsivity and the total noise current are plotted versus the spacing L.

According to fig.4, the noise spectral density S_n changes with I^3 and the scaling law of the corresponding noise current i_n is $I^{3/2}$. Using $I=V/R_s$ (where R_s is the device resistance) and since the $R_s \propto L^2$, an L^{-3} scaling of the noise current is expected. Since the device responsivity is proportional to L^{-2}, according to eq.1, an increase of the detectivity with the finger spacing is expected.

Finally, we observed a small decrease of the detectivity with bias (less than 5%/V). The noise current scaling with bias V is $V^{3/2}$ and the responsivity is directly proportional to V. Therefore a detectivity scaling $\propto V^{-1/2}$ is expected. In the relatively low bias range (0 to 3V) used in this work, the corresponding change is not significant.

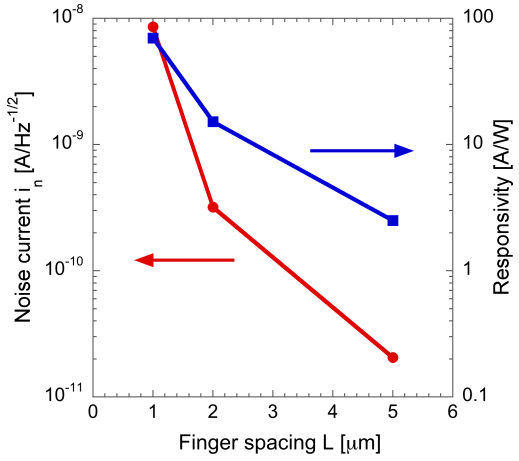

FIG. 6. Total noise current and responsivity vs finger spacing L measured at 1V bias.

In conclusion, we reported on the noise characterization of PbS colloidal quantum dot photoconductors. Noise is clearly dominated by the *1/f* contribution over a wide frequency band, exceeding 1MHz. Despite the large *1/f* noise, specific detectivity exceeding 10^{11} $cmHz^{1/2}W^{-1}$ was obtained at low voltage bias. We observed the noise due to the dark current is different (larger) with respect to the noise due to the photocurrent. We believe this can be associated to the light dependent occupation probability of the trap states, thus suggesting trap engineering can be used to optimize the noise performance. We demonstrated our devices exhibit increased detectivity when operated at lower optical intensity, whereas no significant increase is achieved at larger bias. Finally, we observed larger detectivity is obtained in devices with large finger spacing.

This research was partially funded by EU ACTPHAST project P2014-59. Authors kindly acknowledge Prof. G. Assanto for helpful and stimulating discussions and Prof. S. Tuti from MATCAT Laboratory for help and support with chemical processing.

[1] G. Konstantatos, E.H. Sargent, Infrared Phys. And Technol. **54**, 278 (2011).
[2] X.W. Gong, Z.Y. Yang, G. Walters, R. Comin, Z.J. Ning, V. Adinolfi, O. Voznyy, E.H. Sargent, Nat. Photon. **10**, 253 (2016).
[3] S. Emin, S.P. Singh, L.Y. Han, N. Satoh, A. Islam, Solar Energy. **85**, 1264 (2011).
[4] J.G. He, J. Chen, Y. Yu, L. Zhang, G.Z. Zhang, S.L. Jiang, W. Liu, J. Mater. Sci. **25**, 1499 (2014).
[5] G. Konstantatos, E.H. Sargent, Proc. of the IEEE **97**, 1666 (2009).
[6] E. Lhuillier, S. Keuleyan, P. Guyot-Sionnest, Infrared Phys. And Technol. **59**, 133 (2013).
[7] X. Wang, W. Tian, M. Liao, Y. Bando, D. Golberg, Chem. Soc. Rev. **43**, 1400 (2014).
[8] S. Goossens, G. Navickaite, C. Monasterio, S. Gupta, J. Piqueras, R. Pérez, G. Burwell, I. Nikitskiy, T. Lasanta, T. Galán, E. Puma, A. Centeno, A. Pesquera, A. Zurutuza, G. Konstantatos and F. Koppens, Nat. Photon. **11**, 366 (2017).
[9] R. Saran, R.J. Curry, Nat. Photon. **10**, (2016).
[10] G. Konstantatos, J. Howard, A. Fisher, S. Hoogland, J.P. Clifford, E. Klem, L. Levina, E.H. Sargent, Nature, **442**, 180 (2006).
[11] S. Yakunin, D.N. Dirin, L. Protesescu, M. Sytnyk, S. Tollabimazraehno, M. Humer, F. Hackl, T. Fromherz, M.I. Bodnarchuk, M.V. Kovalenko, W. Heiss, ACS Nano. **8**, 12883 (2014).
[12] C. Giansante, I. Infante, E. Fabiano, R. Grisorio, G. Suranna, G. Gigli, J. Am. Chem. Soc. **137**, 1875 (2015).
[13] F.P. Garcia de Arquer, T. Lasanta, M. Benechea, G. Konstantatos, Small. **11**, 2636 (2015).
[14] R. Saran, V. Stolojan, R.J. Curry, Sci. Rep. **4**, 5041 (2014).
[15] C. Hu, A. Gassenq, Y. Justo, K. Devloo-Casier, H. Chen, C. Detavernier, Z. Hens, G. Roelkens, Appl. Phys. Lett. **105**, 171110 (2014).
[16] A. De Iacovo, C. Venettacci, L. Colace, L. Scopa and S. Foglia, Sci. Rep. **6**, 37913 (2016).
[17] L. Gao, D. Dong, J. He, K. Qiao, F. Cao, M. Li, H. Liu, Y. Cheng, J. Tang, H. Song, Appl. Phys. Lett. **105**, 153702 (2014).
[18] A. De Iacovo, C. Venettacci, L. Colace, L. Scopa, and S. Foglia, IEEE Photon. Technol. Lett. **29**, 703(2017).
[19] Z. Ren, J. Sun, H. Li, P. Mao, Y. Wei, X. Zhong,J. Hu,S. Yang, J. Wang, Adv. Mater. **29**, 1702055 (2017).
[20] J. He, K. Qiao, L. Gao, H. Song, L. Hu, S. Jiang, J. Zhong, J. Tang, ACS Photon. **1**, 936 (2014).
[21] H. Liu, E. Lhuillier, P. Guyot-Sionnest, J. Appl. Phys. **115**, 154309 (2014).
[22] Y. Lai, H. Li, D.K. Kim, B.T. Diroll, C.B. Murray and C.R. Kagan, ACS Nano 8, 9664 (2014).
[23] O. Voznyy, D. Zhitomirsky, P. Stadler, Z. Ning, S. Hoogland, E.A. Sargent, ACS Nano. **6**, 8448 (2012).
[24] J. Liu, in Photonic Devices, Cambridge Univ. Press, p.960 (2010).
[25] K.M. van Kliet, Proc. of the IRE, **46**, 1004 (1958).
[26] A. Van der Ziel, Proc. of the IEEE, **76**, 233 (1988).
[27] C. Kurdak, J,. Kim, A. Kuo, J.J. Lucido, L.A. Farina, X. Bai, M.P. Rowe, A.J. Matzger, Appl. Phys. Lett. 86, 073506 (2005).
[28] E. Lhuillier, S. Keuleyan, H. Liu, P. Guyot-Sionnest, J. Electron. Mater. **41**, 2725 (2012).
[29] W.J. Choi, J.D. Song, S.H. Hwang, J.I. Lee, J.H. Kim, J.I. Song, E.K. Kim, A. Chovet, Physica E **26**, 366 (2005).